

Electromagnetic radiation due to naked singularity formation in self-similar gravitational collapse

Eiji Mitsuda,^{*} Hirotaka Yoshino,[†] and Akira Tomimatsu[‡]
*Department of Physics, Graduate School of Science,
 Nagoya University, Chikusa, Nagoya 464-8602, Japan*

Dynamical evolution of test fields in background geometry with a naked singularity is an important problem relevant to the Cauchy horizon instability and the observational signatures different from black hole formation. In this paper we study electromagnetic perturbations generated by a given current distribution in collapsing matter under a spherically symmetric self-similar background. Using the Green's function method, we construct the formula to evaluate the outgoing energy flux observed at the future null infinity. The contributions from "quasi-normal" modes of the self-similar system as well as "high-frequency" waves are clarified. We find a characteristic power-law time evolution of the outgoing energy flux which appears just before naked singularity formation, and give the criteria as to whether or not the outgoing energy flux diverges at the future Cauchy horizon.

PACS numbers: 04.20.Dw, 04.30.Nk, 02.30.Nw

I. INTRODUCTION

While Penrose has proposed the so-called cosmic censorship conjecture[1], several spacetimes admitting naked singularity formation even in gravitational collapse of physically reasonable matter from regular initial data have been found over the past three decades (see [2, 3] for a recent review). The examples well-studied are spherically symmetric collapses of an inhomogeneous dust ball[4, 5], and a self-similar isothermal gas[6, 7, 8, 9]. A shell-focusing naked singularity can appear at the center in a wide range of the initial data set.

It is an important problem to understand peculiar physical phenomena associated with naked singularity formation. Time evolution of various perturbations in black hole geometry have been extensively studied, and the late-time behaviors such as quasi-normal ringings and power-law tails have been clarified. Such perturbation analysis in background geometry involving a naked singularity will be interesting not only in relation to the possible instability of the Cauchy horizon but also in terms of revealing some typical patterns of time evolution observable as a precursor of naked singularity formation.

The first step to approach this problem will be to consider spherically symmetric self-similar models of gravitational collapse as background spacetime. Because all dimensionless components of the background metric depend only on the one self-similar variable $z \equiv r/t$, the perturbation analysis becomes mathematically simpler. In addition, there exist numerical simulations[10] showing that the geometrical structure and the fluid motion at late stages in general non-self-similar collapse of an isothermal gas can be well described by the general relativistic version[6] of the Larson-Penston self-similar solution. We can expect self-similar solutions to be a realistic model of gravitational collapse.

Several works have been devoted to the analysis of perturbations generated in spherically symmetric self-similar collapse with naked singularity formation. For example, using quantum theory of particle production in curved spacetime, it has been shown that the energy flux of the semiclassical radiation diverges on the Cauchy horizon according to inverse square power-law of the retarded time[11, 12, 13, 14, 15, 16]. On the other hand, considering classical perturbations of a massless scalar field, Nolan and Waters[17] have claimed that the energy flux of scalar perturbations remains finite even at the Cauchy horizon. Their analysis is based on the behavior of perturbations written by $v^n H_n(z)$ with the advanced null coordinate v and a complex parameter n . In this paper we pursue the classical analysis more extensively, by using the Green's function method. Though we use a standard Fourier decomposition of the Green's function by the function $\exp(i\omega \log |t|)$ (in an analogous way to the Mellin transformation in [17]), we reveal time evolution of perturbations by integrating the Fourier components with respect to the spectral parameter ω , which will allow us to find new features missed in [17].

Further we focus our investigation on electromagnetic perturbations generated by any given axisymmetric and circular current distribution in collapsing matter. Of course we must assume that the existence of the source current

^{*}Electronic address: emitsuda@gravity.phys.nagoya-u.ac.jp

[†]Electronic address: yoshino@gravity.phys.nagoya-u.ac.jp

[‡]Electronic address: atomi@gravity.phys.nagoya-u.ac.jp

does not disturb the background self-similar metric. This special choice of a test field is partly motivated by an astrophysical interest related to highly energetic phenomena such as γ -ray bursts (for example, see [18] for electromagnetic radiation in a process of black hole formation). In addition, the mathematical setup of the Green's function method for electromagnetic perturbations becomes quite simpler in comparison with gravitational perturbations. Nevertheless, we would like to mention that the Green's function method developed in the following sections does not essentially rely on a special property of electromagnetic fields. The application to scalar and gravitational perturbations will be straightforward.

In this paper we are mainly concerned with time variation of the outgoing energy flux (namely, the Poynting flux) observed at the future null infinity. In Sec. II, we illustrate spherically symmetric self-similar models admitting naked singularity formation at the center, and we derive the basic equation for a gauge invariant and odd parity electromagnetic perturbation. In Sec. III, we introduce the retarded Green's function and its Fourier decomposition, from which we construct the formula to extract the outgoing wave part of the electromagnetic perturbation propagating to the future null infinity. Contributions from various Fourier components parameterized by ω , (for example, corresponding to high- ω waves, quasi-normal modes of the self-similar system with a complex ω) are clarified in Sec. IV. A characteristic power-law behavior (accompanied with or without an oscillatory behavior) of the outgoing energy flux as a function of the retarded time is found as a signature of naked singularity formation. We obtain in the final section the critical conditions for the self-similar background as to whether or not the outgoing energy flux diverges at the future Cauchy horizon, and a physical interpretation of our results is presented. Throughout this paper, the units in which $c = G = 1$ are used.

II. SETUP OF THE SYSTEM

Let us begin with a brief review of spherically symmetric self-similar collapse with naked singularity formation. The line element of the background spacetime is given by

$$ds^2 = -e^{2\nu} dt^2 + e^{2\lambda} dr^2 + r^2 S^2 (d\theta^2 + \sin^2 \theta d\phi^2), \quad (2.1)$$

with the comoving coordinates t and r . The self-similarity considered here means

$$\nu = \nu(z), \quad \lambda = \lambda(z), \quad S = S(z), \quad (2.2)$$

where $z \equiv r/t$, and the Ricci scalar has the form

$$R = \frac{1}{t^2} \times (\text{function depending only on } z), \quad (2.3)$$

which should grow up as t approaches zero along a $z = \text{constant}$ line. Thus a singularity will appear at the center $r = 0$ at the time $t = 0$. A spacelike singularity may also appear along the $z = z_*$ line where $S(z_*) = 0$.

Using the function defined by

$$V(z) \equiv ze^{\lambda-\nu}, \quad (2.4)$$

the equations for the radial outgoing and ingoing null geodesics are given by

$$\frac{dz}{dt} = \pm \frac{z(1 \pm V)}{tV}. \quad (2.5)$$

The key point is that the $z = \text{constant}$ line giving $V = 1$ (or $V = -1$) becomes a radial outgoing (or ingoing) null geodesic. In order to allow the central singularity to be naked as a result of collapse with regular initial data, in this paper, we assume the schematic behavior of the function $V(z)$ drawn in Fig. 1, for which we obtain the global structure of the self-similar background written in Fig. 2 (see [8] for details of how to construct kinematically the spacetime diagram).

The value of local minimum of V at $z = z_m$ should be less than unity, because the line $z = z_2 > z_m$ giving $V = 1$ becomes the future Cauchy horizon for the null naked singularity corresponding to another root $z = z_3 < z_m$ of $V = 1$. There exist the future null infinity and the event horizon also at the $z = z_2$ and $z = z_3$ null lines, respectively. The equation $V = -1$ has a unique root $z = z_1 < 0$ corresponding to the past Cauchy horizon and the past null infinity. Such a behavior of V as a function of z is found in a wide parameter range of the self-similar metrics describing the collapse of dust or isothermal gas [6, 19, 20, 21].

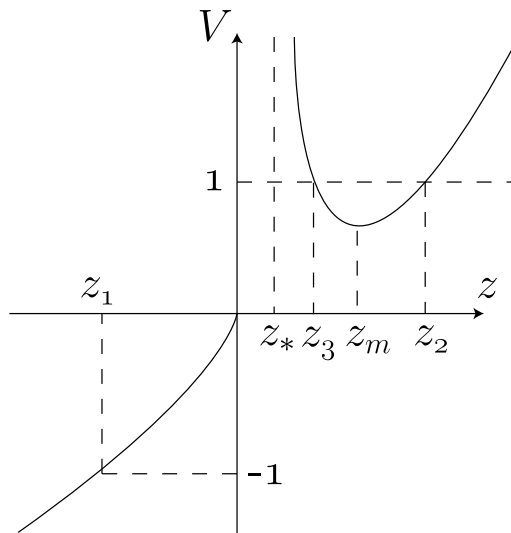


FIG. 1: Schematic description of the function $V(z)$ giving a typical collapse with naked singularity formation. In this figure it should be noted that $V(0) = 0$ and $V \rightarrow \pm\infty$ as $z \rightarrow \pm\infty$.

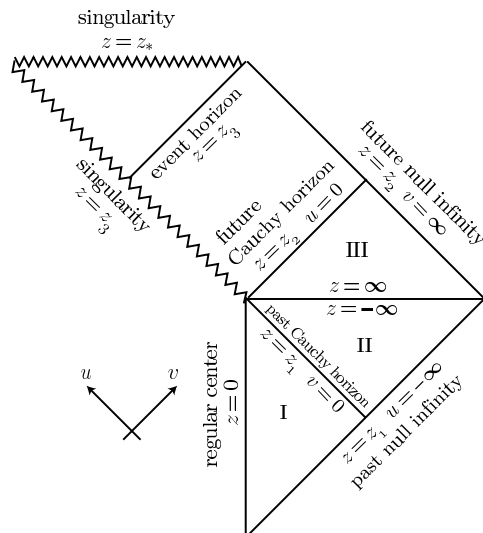


FIG. 2: The Penrose diagram of spacetime corresponding to the function $V(z)$ shown in Fig. 1. The values of the null coordinates u and v are given at some boundaries of the regions I, II and III.

We are interested in time evolution of electromagnetic perturbations in the regions I, II and III shown in Fig. 2. For this purpose it is useful to introduce the retarded and advanced null coordinates u and v . Integrating Eq. (2.5), we obtain

$$u = -|t|e^{h_{\text{out}}(z)}, \quad v = \mp|t|e^{h_{\text{in}}(z)}, \quad (2.6)$$

where $v \leq 0$ in the region I and $v \geq 0$ in the region II and III, while $u \leq 0$ in these regions. The functions $h_{\text{out}}(z)$ and $h_{\text{in}}(z)$ are expressed by

$$h_{\text{out}}(z) = \int \frac{Vdz}{z(V-1)}, \quad h_{\text{in}}(z) = \int \frac{Vdz}{z(V+1)}, \quad (2.7)$$

with the requirement that $h_{\text{out}} = h_{\text{in}} = 0$ at $z = 0$ (namely, $u = v = t < 0$ at the regular center $r = 0$ represented by the $z = 0$ line). We can also note that the null coordinates are given by $u = v = r$ at the spacelike hypersurface $t = 0$ corresponding to the horizontal $z = \pm\infty$ line, which is the boundary between the regions II and III. In the limit

$z \rightarrow z_1$ the function h_{in} is approximately given by

$$h_{\text{in}}(z) \simeq -\frac{1}{z_1 V'(z_1)} \log |z - z_1|. \quad (2.8)$$

Hereafter a prime means the derivative with respect to z . Because $-z_1 V'(z_1)$ is positive (see Fig. 1), the advanced null coordinate v becomes continuously zero, even if not analytically, at the boundary $z = z_1$ (namely, the past Cauchy horizon) between the regions I and II. It remains finite at the past null infinity where $z = z_1$ and $t \sim u = -\infty$. On the other hand, in the limit $z \rightarrow z_2$ we obtain

$$h_{\text{out}}(z) \simeq \frac{1}{z_2 V'(z_2)} \log |z - z_2|. \quad (2.9)$$

Because $z_2 V'(z_2)$ is also positive, the retarded null coordinate u also becomes continuously zero at the boundary $z = z_2$ (namely, the future Cauchy horizon) of the regions III, though it remains finite at the future null infinity where $z = z_2$ and $t \sim v = \infty$. It is easy to check that in the limit $\nu = \lambda = 0$, the coordinates u and v become identical with the usual null coordinates giving the Minkowski metric.

The values of $-z_1 V'(z_1)$ and $z_2 V'(z_2)$ in Eqs. (2.8) and (2.9) will become important to determine the behavior of the outgoing energy flux of the perturbations near the future Cauchy horizon. In the spherically symmetric spacetime written by the self-similar metric (2.2), there exists a homothetic Killing vector field $\chi^a = (-t, -r, 0, 0)$, which satisfies

$$\mathcal{L}_\chi g_{ab} = -2g_{ab}, \quad (2.10)$$

where \mathcal{L}_χ denotes the Lie derivative along the field χ^a (the minus sign of the t and r components of χ^a is chosen so that χ^a points toward the direction toward which the curvature increases[8]). The values of $-z_1 V'(z_1)$ and $z_2 V'(z_2)$ are derived by evaluating the derivative of the inner product of the homothetic Killing vector χ^a on the past Cauchy horizon $z = z_1$ and the future Cauchy horizon $z = z_2$ as follows,

$$\nabla^a (\chi^b \chi_b) = -2\kappa \chi^a, \quad (2.11)$$

where $\kappa = -z_1 V'(z_1)$ on the past Cauchy horizon and $\kappa = z_2 V'(z_2)$ on the future Cauchy horizon. In the stationary black hole geometry, the constant κ evaluated on the event horizon for a Killing field χ^a normal to the horizon has a physical meaning as the surface gravity. Though $-z_1 V'(z_1)$ and $z_2 V'(z_2)$ do not necessarily have such a physical meaning, in this paper we denote $-z_1 V'(z_1)$ and $z_2 V'(z_2)$ by κ_1 and κ_2 , respectively.

Finally in this section we derive the basic equation for electromagnetic perturbations in the self-similar background, by considering the Maxwell equation $\nabla^b (\partial_b A_a - \partial_a A_b) = 4\pi j_a$ for the vector potential A_a . The given source current j_a satisfying the continuity equation $\nabla_a j^a = 0$ is assumed to be axisymmetric and circular, and in order to separate the variable θ , we resolve the source current into spherical harmonics. Then, the multipole component parameterized by $l = 1, 2, \dots$ is given by

$$j_a = \left(0, 0, 0, j_l(t, r) \sin \theta \frac{\partial P_l}{\partial \theta} \right), \quad (2.12)$$

which generates the vector potential A_a (with the angular momentum parameterized by l) of the form

$$A_a = \left(0, 0, 0, a(t, r) \sin \theta \frac{\partial P_l}{\partial \theta} \right), \quad (2.13)$$

according to the equation

$$\hat{L}a(t, z) = -Q_l(t, z), \quad (2.14)$$

where

$$\begin{aligned} \hat{L} = t^2 \frac{\partial^2}{\partial t^2} - 2zt \frac{\partial^2}{\partial t \partial z} - \left(e^{2(\nu-\lambda)} - z^2 \right) \frac{\partial^2}{\partial z^2} + \left\{ 2z + z^2(\lambda' - \nu') - e^{2(\nu-\lambda)}(\nu' - \lambda') \right\} \frac{\partial}{\partial z} \\ - (\lambda' - \nu')zt \frac{\partial}{\partial t} + \frac{e^{2\nu} l(l+1)}{z^2 S^2}, \end{aligned} \quad (2.15)$$

and

$$Q_l(t, z) = 4\pi t^2 e^{2\nu} j_l. \quad (2.16)$$

The current distribution $j_l(t, r)$ in Eq. (2.12) is not specified in this paper, except that it rapidly decreases to zero at the regular center $r = 0$, at spatial infinity $r \rightarrow \infty$ and at distant past $t \rightarrow -\infty$. We will obtain the solution $a(t, z)$ under the boundary condition such that $a(t, z)$ remains regular at the regular center $z = 0$ (and $t < 0$), and there is no ingoing flux from the past null infinity $z = z_1$ (and $t \rightarrow -\infty$). The latter is required to assure us that electromagnetic perturbations are generated through the process of the self-similar gravitational collapse.

III. THE GREEN'S FUNCTION METHOD

As mentioned in Sec. I, the main purpose of this paper is to estimate the outgoing energy flux (the Poynting flux) observed at the future null infinity near the future Cauchy horizon, by solving the wave equation (2.14) for the electromagnetic vector potential $a(t, z)$. Our approach to this problem is to develop the Green's function method useful for the analysis of any test fields in the self-similar background.

Following the standard technique, we give the time evolution of $a(t, z)$ as

$$a(t, z) = \int \int G(t, z|s, y) Q_l(s, y) ds dy, \quad (3.1)$$

with the (time-domain) Green's function $G(t, z|s, y)$, satisfying

$$\hat{L}G(t, z|s, y) = -\delta(t - s)\delta(z - y). \quad (3.2)$$

The causality condition requires that $G = 0$ if the source point represented by the coordinates s and y is located in the exterior of the past light cone of the observation point represented by t and z , in other words, if $u' > u$ or $v' > v$ for the null coordinates defined by $u' \equiv u(s, y)$ and $v' \equiv v(s, y)$.

The key point for analyzing the Green's function is that the differential operator \hat{L} in Eq. (3.2) is invariant under the scale transformation $t \rightarrow kt$ with a parameter k , for which z is fixed. This motivates us to adopt the standard Fourier decomposition of the form

$$G(t, z|s, y) = \frac{1}{2\pi s} \int_{-\infty}^{\infty} \tilde{G}(z, y, \omega) e^{i\omega \log|t/s|} d\omega, \quad (3.3)$$

because Eq. (3.2) reduces to the tractable ordinary differential equation

$$\tilde{G}''(z, y, \omega) + p(z, \omega)\tilde{G}'(z, y, \omega) + q(z, \omega)\tilde{G}(z, y, \omega) = \frac{\delta(z - y)}{e^{2(\nu-\lambda)}(1 - V^2)}, \quad (3.4)$$

where the coefficients are given by

$$p(z, \omega) = \frac{2(i\omega - 1)z + (\nu' - \lambda')e^{2(\nu-\lambda)}(1 + V^2)}{e^{2(\nu-\lambda)}(1 - V^2)}, \quad (3.5)$$

and

$$q(z, \omega) = \frac{\omega(i + \omega)S^2 z^2 - i\omega(\nu' - \lambda')S^2 z^3 - e^{2\nu}l(l + 1)}{S^2 z^2 e^{2(\nu-\lambda)}(1 - V^2)}. \quad (3.6)$$

The spectral parameter ω introduced here may be regarded as a wave frequency in the lapse of the logarithmic time $\log|t|$. Hence, hereafter we will call $\tilde{G}(z, y, \omega)$ the frequency-domain Green's function as usual.

It is straightforward to construct the frequency-domain Green's function by the help of two independent homogeneous solutions for Eq. (3.4). If the boundary condition mentioned in the previous section is imposed on $a(t, z)$, one of the homogeneous solution denoted by $\psi_0(z, \omega)$ should be regular at the regular center $z = 0^-$, while the other denoted by $\psi_{\text{out}}(z, \omega)$ should be purely outgoing at $z = z_1 < 0$ to assure the absence of ingoing waves originated from the past null infinity. Then, we have

$$\tilde{G}(z, y, \omega) = \begin{cases} \tilde{G}_1(z, y, \omega) = \psi_{\text{out}}(z, \omega)\psi_0(y, \omega)/\bar{W}(y, \omega) & \text{for } z < y, \\ \tilde{G}_2(z, y, \omega) = \psi_0(z, \omega)\psi_{\text{out}}(y, \omega)/\bar{W}(y, \omega) & \text{for } z > y, \end{cases} \quad (3.7)$$

where the common factor $\bar{W}(y, \omega) = w(\omega)e^{\nu(y)-\lambda(y)}e^{i\omega h_{\text{in}}(y)}e^{i\omega h_{\text{out}}(y)}$ is derived from the Wronskian

$$\psi_{\text{out}}\psi_0' - \psi_0\psi_{\text{out}}' = w(\omega) \exp\left(-\int p(z', \omega) dz'\right) = \frac{\bar{W}}{e^{2(\nu-\lambda)}(1 - V^2)}, \quad (3.8)$$

with $w(\omega)$ independent of z .

If a homogeneous solution which becomes purely ingoing at $z = z_1$ is denoted by $\psi_{\text{in}}(z, \omega)$, the mode ψ_0 regular at $z = 0^-$ may be written by the sum

$$\psi_0(z, \omega) = \psi_{\text{out}}(z, \omega) + \psi_{\text{in}}(z, \omega). \quad (3.9)$$

In this paper we claim the wave modes ψ_{out} and ψ_{in} to become purely outgoing and ingoing, respectively, at $z = z_1$ in the sense that they can be expressed by the WKB forms

$$\psi_{\text{out}}(z, \omega) = g_{\text{out}}(z, \omega) \exp\{i\omega h_{\text{out}}(z)\}, \quad \psi_{\text{in}}(z, \omega) = g_{\text{in}}(z, \omega) \exp\{i\omega h_{\text{in}}(z)\}, \quad (3.10)$$

with the amplitudes g_{out} and g_{in} ‘‘regular’’ at $z = z_1$ (where $V = -1$ and $h_{\text{in}} \rightarrow -\infty$). However, in general, we cannot expect that g_{out} and g_{in} remain regular at another regular singular point $z = z_2$ (where $V = 1$ and $h_{\text{out}} \rightarrow -\infty$) in Eq. (3.4). For example, g_{out} may contain a term with the oscillatory factor $\exp(-i\omega h_{\text{out}})$ which becomes singular in the limit $z \rightarrow z_2$. This corresponds to a partial conversion of outgoing waves into ingoing ones in the propagation from the past Cauchy horizon $z = z_1$ toward the future null infinity $z = z_2$, and may be interpreted as a result of back scattering effect of spacetime curvature. (In the later discussion we will take account of this mode conversion to estimate electromagnetic radiation observed at the future null infinity.) Then, denoting two independent modes which become purely outgoing and ingoing at $z = z_2$ by $\bar{\psi}_{\text{out}}$ and $\bar{\psi}_{\text{in}}$, respectively, we obtain

$$\psi_{\text{out}}(z, \omega) = b_1(\omega)\bar{\psi}_{\text{out}}(z, \omega) + b_2(\omega)\bar{\psi}_{\text{in}}(z, \omega), \quad (3.11)$$

with some coefficients b_1 and b_2 dependent on ω . These new modes $\bar{\psi}_{\text{out}}$ and $\bar{\psi}_{\text{in}}$ also can be written as

$$\bar{\psi}_{\text{out}} = \bar{g}_{\text{out}}(z, \omega) \exp\{i\omega h_{\text{out}}(z)\}, \quad \bar{\psi}_{\text{in}} = \bar{g}_{\text{in}}(z, \omega) \exp\{i\omega h_{\text{in}}(z)\}, \quad (3.12)$$

with the amplitudes \bar{g}_{out} and \bar{g}_{in} regular at $z = z_2$, and the relation

$$\psi_0(z, \omega) = \bar{\psi}_{\text{out}}(z, \omega) + \bar{\psi}_{\text{in}}(z, \omega), \quad (3.13)$$

is also assumed for their normalization.

Now let us present a more definite expression of the double integral in Eq. (3.1) over the regions I, II and III shown in Fig. 2. Recall that the frequency-domain Green’s function $\tilde{G}(z, y, \omega)$ is constructed under the conditions at the inner boundary $z = 0$ and the outer one $z = z_1$ surrounding the region I. Then, if the observation point (t, z) is located in the region I, the solution $a(t, z)$ can be written as

$$a(t, z) = \int_0^z dy \int_{-\infty}^{s_1} ds G_1(t, z|s, y) Q_I(s, y) + \int_z^{z_1} dy \int_{-\infty}^{s_2} ds G_2(t, z|s, y) Q_I(s, y), \quad (3.14)$$

where $G_1(t, z|s, y)$ and $G_2(t, z|s, y)$ are given by the Fourier-type integral (3.3) of the frequency-domain Green’s functions $\tilde{G}_1(z, y, \omega)$ and $\tilde{G}_2(z, y, \omega)$, respectively. From the causality condition the upper limits $s_1(u, y)$ and $s_2(v, y)$ in the integrals with respect to s should be determined by the relations $u(t, z) = u'(s_1, y)$ and $v(t, z) = v'(s_2, y)$. Note that the integral of the second term of the right hand side with respect to s approaches the integral in the range from $s = -\infty$ to $s = t$ as $z \rightarrow z_1$ (and $v \rightarrow 0$).

The integral representation (3.14) assures the absence of unphysical ingoing radiation which may make the solution $a(t, z)$ singular at the past Cauchy horizon $z = z_1$ (or $v = 0$), where the second term (including G_2) vanishes, and owing to the relation $\tilde{G}_1 \sim \psi_{\text{out}}(z, \omega)$ the first term (including G_1) becomes regular. This regularity of $a(t, z)$ at the outer boundary $z = z_1$ of the region I allows us to extrapolate Eq. (3.14) to the form valid at the observation point (t, z) located in the region II where $-\infty \leq z \leq z_1$ and $t \leq 0$ as follows,

$$\begin{aligned} a(t, z) &= \int_0^{z_1} dy \int_{-\infty}^{s_1} ds G_1(t, z|s, y) Q_I(s, y) \\ &+ \int_{z_1}^z dy \int_{s_2}^{s_1} ds \{G_1(t, z|s, y) - G_2(t, z|s, y)\} Q_I(s, y). \end{aligned} \quad (3.15)$$

The first term in Eq. (3.15) corresponds to the contribution from the source point (s, y) located in the region I, while the second one corresponds to the contribution from the source point located in the region II. Note that the integral of the second term with respect to s is limited to the range $s_2 \leq s \leq s_1$ by virtue of the causality condition, and approaches the integral in the range from $s = -\infty$ to $s = t$ as $z \rightarrow z_1$ (and $v \rightarrow 0$) to allow us to continuously shift from the integral representation (3.14) to that of Eq. (3.15) beyond $v = 0$.

The next step is to extrapolate Eq. (3.15) to the form valid in the observation point (t, z) located in the region III where $+\infty \geq z \geq z_2$ and $t \geq 0$. As shown in Fig. 2, the boundary between the regions II and III is given by the $z = \pm\infty$ line. This change of the sign of the variables z (and t) is not troublesome for the continuous extrapolation of Eq. (3.15), because we obtain

$$\psi_{\text{out}}(z, \omega) \exp(i\omega \log |t|) \sim \psi_{\text{in}}(z, \omega) \exp(i\omega \log |t|) \sim \exp(i\omega r), \quad (3.16)$$

in the limit $z \rightarrow \pm\infty$ where we use $V \rightarrow \pm\infty$ in Eq. (2.7). (The amplitudes $g_{\text{out}}(z, \omega)$ and $g_{\text{in}}(z, \omega)$ are also continuous at the boundary $z = \pm\infty$.) Hence, Eq. (3.15) holds in the region III without any modifications, except that the integral in the second term of the right-hand side should be understood as the contribution from the source point (s, y) located in the regions II and III.

To clarify the physical properties of the solution $a(t, z)$, it will be convenient to use the null coordinates u and v for the observation point and u' and v' for the source point. This coordinate transformation gives the Jacobian

$$\left| \frac{\partial(s, y)}{\partial(u', v')} \right| \equiv J(u', v') = \frac{sy(1 - V^2(y))}{2V(y)u'v'}, \quad (3.17)$$

and Eqs. (3.14) and (3.15) are rewritten into the unified form

$$a(u, v) = \int_{-\infty}^u du' \int_{u'}^v dv' H(u, v|u', v') Q_l(u', v') J(u', v'), \quad (3.18)$$

where the lower limit of the integral with respect to v' should be u' , because the regular center $y = 0$ corresponds to $v' = u'$. If the observation point (u, v) is located in the region I, the function $H(u, v|u', v')$ in Eq. (3.18) is equal to the original Green's function $G(t, z|s, y)$. However, if the observation point (u, v) is located in the region II (or in the region III), we obtain

$$H(u, v|u', v') = G_1(t, z|s, y), \quad (3.19)$$

for the source point (u', v') located in the region I, and

$$H(u, v|u', v') = G_1(t, z|s, y) - G_2(t, z|s, y), \quad (3.20)$$

for the source point (u', v') located in the region II (or in the regions II and III). The validity of the integral representation (3.18) is supported in Appendix A, by applying this formula to a static field $a(t, z) = a(r)$ in the Minkowski background.

Our main concern in this paper is the emission of outgoing radiation toward the future null infinity. Hence, using the two modes $\bar{\psi}_{\text{out}}(z, \omega)$ and $\bar{\psi}_{\text{in}}(z, \omega)$ instead of $\psi_{\text{out}}(z, \omega)$ and $\psi_{\text{in}}(z, \omega)$, we divide the frequency-domain Green's function given by Eq. (3.7) into the outgoing and ingoing wave parts as follows,

$$\tilde{G}_\gamma(z, y, \omega) = \bar{\psi}_{\text{out}}(z, \omega) \tilde{G}_{\gamma\text{out}}(y, \omega) + \bar{\psi}_{\text{in}}(z, \omega) \tilde{G}_{\gamma\text{in}}(y, \omega), \quad (3.21)$$

where $\gamma = 1, 2$. The outgoing part of the right-hand side of Eq. (3.21) can derive the ‘‘retarded’’ Green's functions $G_{\gamma\text{out}}(u, v|u', v')$ as

$$G_{\gamma\text{out}}(u, v|u', v') = \frac{1}{2\pi s} \int_{-\infty}^{\infty} \bar{\psi}_{\text{out}}(z, \omega) \tilde{G}_{\gamma\text{out}}(y, \omega) e^{i\omega \log(t/|s|)} d\omega, \quad (3.22)$$

which reduces to

$$G_{\gamma\text{out}}(u|u', v') = \frac{1}{2\pi s} \int_{-\infty}^{\infty} \bar{g}_{\text{out}}(z_2, \omega) \tilde{G}_{\gamma\text{out}}(y, \omega) e^{i\omega \log(-u/|s|)} d\omega, \quad (3.23)$$

in the limit $v \rightarrow \infty$ (i.e., $z \rightarrow z_2$) with a fixed u . Via the above-mentioned procedure and Eq. (3.18) we can obtain the outgoing part $a_{\text{out}}(u, v)$ of the vector potential $a(u, v)$. The final formula for the outgoing radiation field $a_{\text{out}}(u) \equiv a_{\text{out}}(u, z_2)$ observed at the future null infinity $v \rightarrow \infty$ (i.e., $z \rightarrow z_2$) is given by

$$a_{\text{out}}(u) = \int_{-\infty}^u du' \int_{u'}^{\infty} dv' H_{\text{out}}(u|u', v') Q_l(u', v') J(u', v'), \quad (3.24)$$

where $H_{\text{out}}(u|u', v')$ is equal to $G_{1\text{out}}(u|u', v')$ for the source point (u', v') located in the region I, and is equal to $G_{1\text{out}}(u|u', v') - G_{2\text{out}}(u|u', v')$ for the source point (u', v') located in the regions II and III. The explicit form may be written by

$$H_{\text{out}}(u|u', v') = \frac{1}{2\pi s e^{\nu(y)-\lambda(y)}} \int_{-\infty}^{\infty} \frac{\bar{g}_{\text{out}}(z_2, \omega)}{w(\omega)} \left\{ K(y, \omega) e^{i\omega \log(-u/|v'|)} + N(y, \omega) e^{i\omega \log(u/u')} \right\} d\omega, \quad (3.25)$$

where

$$K = 0, \quad N = (b_1 - b_2) \bar{g}_{\text{in}}(y, \omega), \quad (3.26)$$

in the range $v' \geq -u'$ (i.e., in the region III). If the source point is located in the region I or II, the functions K and N should be expressed by $g_{\text{out}}(y, \omega)$ and $g_{\text{in}}(y, \omega)$ instead of $\bar{g}_{\text{out}}(y, \omega)$ and $\bar{g}_{\text{in}}(y, \omega)$ to be regular at the boundary $y = z_1$ (i.e., $v' = 0$). Hence, we obtain

$$K = (b_1 - 1)g_{\text{out}}(y, \omega), \quad N = b_1 g_{\text{in}}(y, \omega), \quad (3.27)$$

in the range $0 \leq v' \leq -u'$ (i.e., in the region II), and

$$K = b_1 g_{\text{out}}(y, \omega), \quad N = b_1 g_{\text{in}}(y, \omega), \quad (3.28)$$

in the range $u' \leq v' \leq 0$ (i.e., in the region I). It should be also remarked that from the causality condition we can use Eq. (3.25) only in the range $u' \leq u$ for the retarded time u' of the source point.

Because the physical quantity to be observable is the energy flux of the outgoing radiation, we must calculate the derivative of $a(u)$ with respect to the retarded time u . Here, for later convenience, we denote the derivative with respect to $\log(-u)$ by a dot, and we have

$$\dot{a}_{\text{out}}(u) = \Psi(u) + \Phi(u), \quad (3.29)$$

where

$$\Psi(u) = \int_{-\infty}^u du' \int_{u'}^{\infty} dv' \dot{H}_{\text{out}}(u|u', v') Q_l(u', v') J(u', v'), \quad (3.30)$$

and

$$\Phi(u) = u \int_u^{\infty} dv' H_{\text{out}}(u|u, v') Q_l(u, v') J(u, v'). \quad (3.31)$$

The future Cauchy horizon due to naked singularity formation appears on the boundary $z = z_2$ (i.e., at the retarded time $u = 0$) of the region III. Hence, to understand clearly a distinctive effect of the naked singularity, our task in the following sections is to investigate the asymptotic behavior of $\dot{a}_{\text{out}}(u)$ in the limit $u \rightarrow 0$ for clarifying whether or not a burst-type emission of the infinite energy flux can occur in the self-similar collapse.

IV. DECOMPOSITION OF CONTRIBUTIONS TO THE GREEN'S FUNCTION

Now let us try to obtain explicitly the asymptotic behavior of the functions $\Psi(u)$ and $\Phi(u)$ in the limit $u \rightarrow 0$ according to the formalism given in the previous section. The first step would be to calculate the integral with respect to ω in Eq. (3.25), by considering the analytic structure of the Wronskian factor w in Eq. (3.8) as a function of ω . Hence, following the analysis of test fields in black hole background, we decompose the Green's function into several distinct parts corresponding to contributions from high-frequency waves with $|\omega| \rightarrow \infty$ and "quasi-normal" modes of the system with complex frequencies giving $w = 0$.

A. High-frequency contribution

In the high-frequency limit $|\omega| \rightarrow \infty$ we can apply the WKB approximation to obtain the homogeneous solutions for Eq. (3.4), and at the leading order the amplitudes $g_{\text{out}}(z, \omega)$ and $g_{\text{in}}(z, \omega)$ are found to become constants denoted here by c_{out} and c_{in} , respectively, without a mode mixing (i.e., $b_1 \simeq 1$, $b_2 \simeq 0$). Then, the Wronskian factor w is approximately given by

$$w(\omega) \simeq 2i\omega c_{\text{out}} c_{\text{in}}. \quad (4.1)$$

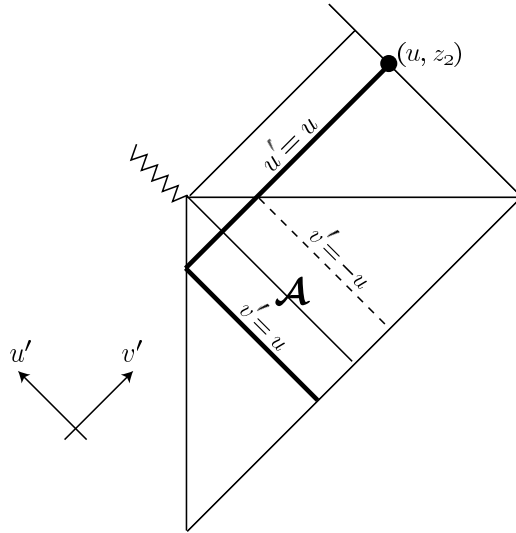


FIG. 3: The source region shown in the Penrose diagram, which is given by the null coordinates u' and v' . The null geodesics $v' = u$ and $u' = u$ starting from the past null infinity and arriving at the observation point denoted by (u, z_2) are shown by the thick solid lines. The broken line corresponds to the $v' = -u$ line. The boundaries of the source region \mathcal{A} are given by $u' = -\infty$, $v' = u$, $u' = u$ and $v' = -u$.

It becomes easy to calculate the derivative of H_{out} with respect to $\log(-u)$ (denoted by $\dot{H}_{\text{out}}^{(F)}$) under this approximation, and we have

$$\dot{H}_{\text{out}}^{(F)}(u|u', v') = \frac{1}{2se^{\nu(y)-\lambda(y)}} \left\{ \frac{c_{\text{out}}}{c_{\text{in}}} \delta\left(\log\left(\frac{u}{v'}\right)\right) + \delta\left(\log\left(\frac{u}{u'}\right)\right) \right\}, \quad (4.2)$$

which is applied to the estimation of $\Psi(u)$ in Eq. (3.30). Denoting the high-frequency part of Ψ by Ψ_F , we arrive at the result such that $\Psi_F(u) = \Psi_{F1}(u) + \Psi_{F2}(u)$, where

$$\Psi_{F1}(u) = \frac{c_{\text{out}}u}{2c_{\text{in}}} \int_{-\infty}^u \bar{Q}_l(u', u) J(u', u) du', \quad \Psi_{F2}(u) = \frac{u}{4} \int_u^{\infty} \bar{Q}_l(u, v') J(u, v') dv', \quad (4.3)$$

with the integrand factor \bar{Q}_l defined by $\bar{Q}_l \equiv Q_l/se^{\nu-\lambda} = 4\pi se^{\nu+\lambda} j_l$ for a given current distribution j_l .

High-frequency waves will be able to propagate without scattering due to the spacetime curvature and the centrifugal barrier (depending on l). In fact, the δ -functions which appear in Eq. (4.2) allow us to use the approximation of geometrical optics for the propagation of high-frequency waves to the future null infinity at the retarded time u (along the path drawn in Fig. 3). The source points (u', v') giving the first term Ψ_{F1} in Ψ_F are located on the ingoing null line $v' = u$. Hence, the outgoing flux represented by Ψ_{F1} is a result of the reflection (at the regular center $v' = u' = u$) of ingoing null rays propagating along $v' = u$, which are generated by the current distribution j_l at the source points (u', u) ranging from $u' \rightarrow -\infty$ to $u' = u$. On the other hand the second term Ψ_{F2} represents the outgoing flux which is generated by the current distribution j_l just on the past null cone $u' = u$ (ranging from $v' = u$ to $v' \rightarrow \infty$) and is directly propagating to the observation point. If the retarded time u of observation at the future null infinity is nearly equal to zero, the source points for Ψ_{F1} (or Ψ_{F2}) on the ingoing null line $v' = u$ (or the outgoing one $u' = u$) become nearly identical with the past (or future) Cauchy horizon, where we obtain roughly $u' \sim s$ (or $v' \sim s$) except an unimportant constant factor. Then, the Jacobians J in the integrands of Eq. (4.3) are roughly given by

$$J(u', u) \sim \frac{1}{u} \left(\frac{u}{u'}\right)^{\kappa_1}, \quad J(u, v') \sim \frac{1}{u} \left(\frac{-u}{v'}\right)^{\kappa_2}, \quad (4.4)$$

where κ_1 and κ_2 are the values previously defined in Sec. II. Hence we obtain

$$\Psi_{F1}(u) \sim (-u)^{\kappa_1} \int_{-\infty}^u j_l(u', z_1) (-u')^{1-\kappa_1} du', \quad \Psi_{F2}(u) \sim (-u)^{\kappa_2} \int_u^{\infty} j_l(v', z_2) v'^{1-\kappa_2} dv'. \quad (4.5)$$

As was mentioned in Sec. II, we assume a rapid decrease of the current distribution j_l near the regular center. A plausible choice would be that $j_l(s, y) \simeq h(s)r^2(s, y)S^2(y)$ at the source point $r = sy \simeq 0$, where $h(s)$ is introduced

as some amplification of j_l in the process of the self-similar collapse. It may be interesting to consider the case that $j_l(s, y)$ diverges at the onset $s = 0$ of the naked singularity for a fixed nonzero y (namely, $hs^2 \rightarrow \infty$ as $s \rightarrow 0$). However, our purpose in this paper is to pursue the possibility of amplified generation of electromagnetic radiation due to the self-similar dynamics of background geometry involving a naked singularity, which requires us to calculate Ψ_{F1} and Ψ_{F2} without any divergence of the source current j_l . (Hereafter we assume h to be finite at $s = 0$ for simplifying our discussion.) Furthermore, we obtain the relations

$$\kappa_1 = 1 - \frac{u^2 R_{uu}}{8}, \quad \kappa_2 = 1 - \frac{v^2 R_{vv}}{8}, \quad (4.6)$$

where R_{vv} and R_{uu} are the components of the Ricci tensor evaluated at $z = z_1$ and $z = z_2$, respectively. Then, if the strong energy condition holds for collapsing matter, we can require the inequality

$$\kappa_1 \leq 1, \quad \kappa_2 \leq 1, \quad (4.7)$$

to show that the integrals in Eq. (4.5) converge even in the limit $u \rightarrow 0$. (Of course, it should be also assumed that the current distribution j_l rapidly decreases as the source point becomes close to the past or future null infinity $u' \rightarrow -\infty$ or $v' \rightarrow \infty$). Hence, finally we find the asymptotic power-law behaviors of Ψ_{F1} and Ψ_{F2} giving the outgoing flux of high-frequency waves to be

$$\Psi_{F1}(u) \sim (-u)^{\kappa_1}, \quad \Psi_{F2}(u) \sim (-u)^{\kappa_2}, \quad (4.8)$$

in the limit $u \rightarrow 0$.

Here let us turn our attention to the additional term $\Phi(u)$ in Eq. (3.29). Note that the source points (u', v') giving $\Phi(u)$ are also located on the past null cone $u' = u$ in the same way as Ψ_{F2} in Eq. (4.3) for high-frequency waves. The contribution to $\Phi(u)$ given at the retarded time u will represent outgoing waves generated on the past null cone ranging from $v' = u$ to $v' \rightarrow \infty$. This allows us to estimate easily the asymptotic behavior of $\Phi(u)$ in the limit $u \rightarrow 0$ without using the high-frequency approximation. The key point is that in the limit $u \rightarrow 0$ the range of the past null cone in the regions I and II shrinks to zero (see Fig. 3). Hence, using Eq. (3.25) valid in the region III, the function $H_{\text{out}}(u|u, v')$ in Eq. (3.31) can be given by

$$H_{\text{out}}(u|u, v') = \frac{I}{2\pi s e^{\nu(z_2) - \lambda(z_2)}}, \quad I = \int_{-\infty}^{\infty} \frac{(b_1 - b_2)}{w(\omega)} \bar{g}_{\text{out}}(z_2, \omega) \bar{g}_{\text{in}}(z_2, \omega) d\omega. \quad (4.9)$$

in the limit $u \rightarrow 0$, where $s \sim v'$ and $y = z_2$ for the source point $u' = 0$. The convergence of the integral I with respect to ω in Eq. (4.9) may be subtle, because the integrand is proportional to $1/\omega$ in the high-frequency limit. However, the contribution of such a high-frequency part can be canceled out, for example, if the infinite integral of any function $\sigma(\omega)$ is defined as

$$\int_{-\infty}^{\infty} \sigma(\omega) d\omega \equiv \lim_{\omega_0 \rightarrow \infty} \int_{-\omega_0}^{\omega_0} \sigma(\omega) d\omega. \quad (4.10)$$

By virtue of such a regularization of the integral we obtain

$$\Phi(u) = \frac{2I}{\pi} \Psi_{F2}(u) \sim (-u)^{\kappa_2}, \quad (4.11)$$

in the limit $u \rightarrow 0$. If wave frequencies are not so large, outgoing waves will be efficiently back-scattered, and their contribution to the function $H_{\text{out}}(u|u, v')$ in $\Phi(u)$ becomes important to estimate the value of I . Nevertheless, from Eq. (4.11) we can conclude that such a back-scattering effect is not relevant to the asymptotic power-law behavior of $\Phi(u)$ which becomes identical with that of $\Psi_{F2}(u)$.

B. Contribution from poles in the Green's function

The frequency-domain Green's function may contain singularities in the complex ω -plane. In black hole background it is well-known that late-time tails of massless test fields are generated by a low-frequency contribution to the frequency-domain Green's function, which appears as a $\omega = 0$ branch cut in the Wronskian factor $w(\omega)$. There may be also a branch cut in the frequency-domain Green's function (3.7) considered here. However, in this paper we do not pursue such a problem. Here our investigation is focused on the pole contribution to $\Psi(u)$, which will be interesting as

a resonant behavior of test fields in the self-similar background. We use the residue calculus to evaluate the integral (with respect to ω) in \dot{H}_{out} , from which the high-frequency part $\dot{H}_{\text{out}}^{(F)}$ is subtracted.

Recall that the simple poles in the frequency-domain Green's function are given by the zeros of $w(\omega)$. We must remark that even in the Minkowski background there are zeros at $\omega = \pm i$ (see Appendix A), and the two mode functions $\psi_{\text{out}}(z, \pm i)$ and $\psi_{\text{in}}(z, \pm i)$ given at the frequencies can satisfy the relation $\psi_0 = \psi_{\text{out}} + \psi_{\text{in}} = 0$. (There is also a zero of w at $\omega = 0$, but it is not a pole because the factor ω in w is canceled out by virtue of the differentiation of Eq. (3.25) with respect to $\log(-u)$.) As shown in Appendix B through the analysis of ψ_{out} and ψ_{in} near $z = z_1$, if the background spacetime is dynamical, the zeros of $w(\omega)$ should change to $\omega = \pm \kappa_1 i$ (note that the value of κ_1 becomes unity in the limit to the Minkowski background). From the same analysis of the different pair given by Eq. (3.12) near $z = z_2$ it is easy to see that the outgoing mode $\bar{\psi}_{\text{out}}$ remains linearly independent of the ingoing mode $\bar{\psi}_{\text{in}}$ at the frequencies $\omega = \pm \kappa_1 i$, because in general the equality $\kappa_1 = \kappa_2$ does not hold. Hence, the requirement such that $0 = \psi_0 = \psi_{\text{out}} + \psi_{\text{in}} = \bar{\psi}_{\text{out}} + \bar{\psi}_{\text{in}} = 0$ at $\omega = \pm \kappa_1 i$ can become consistent only if both $\bar{g}_{\text{out}}(z, \pm \kappa_1 i)$ and $\bar{g}_{\text{in}}(z, \pm \kappa_1 i)$ vanish at any z (in the same way as ψ_0). It is also required that the coefficients b_1 and b_2 in Eq. (3.11) must be inversely proportional to the factor $\omega^2 + \kappa_1^2$ for keeping the functions $g_{\text{out}}(z, \omega)$ and $g_{\text{in}}(z, \omega)$ finite even at $\omega = \pm \kappa_1 i$ (namely, $b_1 \bar{g}_{\text{out}}$ and $b_2 \bar{g}_{\text{in}}$ become finite in the limit $\omega \rightarrow \pm \kappa_1 i$). Then, the residue calculus of Eq. (3.25) for the zeros of w at $\omega = \pm \kappa_1 i$ leads to the result that the pole contributions (denoted by $\dot{H}_{\text{out}}^{(+)}$ and $\dot{H}_{\text{out}}^{(-)}$) to \dot{H}_{out} exist only for the source point located in the range $|v'| < |u| < |u'|$ (namely, in the region \mathcal{A} drawn in Fig. 3), and they are written by

$$\dot{H}_{\text{out}}^{(\pm)}(u|u', v') = \mp \frac{\kappa_1 i \lim^{\pm} \{b_1(\omega) \bar{g}_{\text{out}}(z_2, \omega)\} g_{\text{out}}(y, \pm \kappa_1 i)}{se^{\nu(y) - \lambda(y)} w'(\pm \kappa_1 i)} \times \left(\frac{|v'|}{-u} \right)^{\pm \kappa_1}, \quad (4.12)$$

where $w' = dw/d\omega$, \lim^{\pm} means the limit $\omega \rightarrow \pm \kappa_1 i$, and the relation

$$g_{\text{out}}(y, \pm \kappa_1 i) |u'|^{\mp \kappa_1} = -g_{\text{in}}(y, \pm \kappa_1 i) |v'|^{\mp \kappa_1}, \quad (4.13)$$

is used.

Though the physical interpretation of the modes satisfying the relation $\psi_{\text{out}} = -\psi_{\text{in}}$ at $\omega = \pm \kappa_1 i$ is unclear, their contribution giving $\dot{H}_{\text{out}}^{(\pm)}$ represents a prompt emission of outgoing waves in the region \mathcal{A} including the past Cauchy horizon. In particular, for the growing mode with $\text{Im}(\omega) = \kappa_1 > 0$ the function $H_{\text{out}}^{(+)} (\propto u^{-\kappa_1})$ can infinitely increase as the retarded time u of the observation point approaches zero. However, the source region in the range $u < v' < -u$ is restricted to the past Cauchy horizon in the limit $u \rightarrow 0$, and the $\omega = \kappa_1 i$ contribution (denoted by Ψ_+) to $\Psi(u)$ in Eq. (3.30) turns out to have the asymptotic behavior

$$\Psi_+(u) \sim (-u)^{\kappa_1}, \quad (4.14)$$

because the Jacobian is given by $J(u', v') \sim (1/v')(v'/u')^{\kappa_1}$ near $v' = 0$, and $g_{\text{out}}(y, \kappa_1 i)$ is finite at $y = z_1$ (see Appendix B). This is quite similar to the high-frequency contribution Ψ_{F1} , which is a result of the reflection of an ingoing flux (generated on the null line $v' = u$) just at the regular center $u' = v' = u$. The $\omega = \kappa_1 i$ contribution also may be a result of the conversion of an ingoing flux (generated in the region \mathcal{A}) into an outgoing flux, which occurs on the null line $u' = u$ with the finite range $u < v' < -u$.

In the calculation of the contribution (denoted by Ψ_-) from the decaying mode with $\text{Im}(\omega) = -\kappa_1 < 0$, we must remark that $g_{\text{in}}(y, -\kappa_1 i)$ is finite at $y = z_1$ (see Appendix B), thus from Eq. (4.13) $g_{\text{out}}(y, -\kappa_1 i) \sim |v'/u'|^{\kappa_1}$ near $v' = 0$. Then, we find the asymptotic behavior such that $\Psi_-(u) \sim (-u)^{2\kappa_1}$ in the limit $u \rightarrow 0$. It is obvious that this $\omega = -\kappa_1 i$ contribution becomes unimportant in comparison with Ψ_+ .

In the above-mentioned analysis we have revealed the contributions from various source points located in the range $u \leq v' < \infty$ to the outgoing flux observed at the future null infinity. It is shown here that we can also obtain a contribution from the source point located in the range $u' \leq v' < u$ corresponding to the inner part of the region I, if there exist quasi-normal modes of the dynamical self-similar system with complex frequencies giving $w(\omega) = 0$, at which the function $\psi_{\text{out}}(z, \omega)$ outgoing at $z = z_1$ becomes regular at the regular center $z = 0$. Namely, we assume the relation $\psi_{\text{in}} = \psi_0 - \psi_{\text{out}} = 0$ at $\omega = \omega_q$ ($q = 1, 2, \dots$), instead of the relation $\psi_0 = 0$ at $\omega = \pm \kappa_1 i$.

The real part of ω_q for such quasi-normal modes may be nonzero, and it is proved in Appendix B that the imaginary part of ω_q should be negative. Further, from Eqs. (3.11) and (3.13), the condition $\psi_{\text{in}} = 0$ leads to the result such that $b_1 = b_2 = 1$. Then, using Eq. (3.25) and the residue calculus associated with these poles, we obtain the $\omega = \omega_q$ contribution (denoted by $\dot{H}_{\text{out}}^{(q)}$) to \dot{H}_{out} as follows,

$$\dot{H}_{\text{out}}^{(q)}(u|u', v') = -\frac{\omega_q \bar{g}_{\text{out}}(z_2, \omega_q) g_{\text{out}}(y, \omega_q)}{se^{\nu(y) - \lambda(y)} w'(\omega_q)} \times \left(\frac{u}{v'} \right)^{i\omega_q}. \quad (4.15)$$

Note that Eq. (4.15) is valid only in the range $u' \leq v' < u$, and $\dot{H}_{\text{out}}^{(q)} = 0$ at any other source points in the regions I, II and III. The quasi-normal modes represent a disturbance excited in the inner region around the regular center, which can generate outgoing waves arriving at the future null infinity.

The key point to calculate the contribution (denoted by Ψ_q) from the quasi-normal modes to $\Psi(u)$ is that the integral in Eq. (3.30) with respect to v' is limited to the range $u' \leq v' \leq u$, and the integrand becomes proportional to the factor $|v'|^{-i\omega_q + \kappa_1 - 1}$ in the limit $v' \rightarrow 0$. Then, it is easy to see that the asymptotic behavior of Ψ_q in the limit $u \rightarrow 0$ is given by

$$\Psi_q(u) \sim (-u)^{i\omega_q}, \quad (4.16)$$

if the quasi-normal mode decays slowly (namely, $|\text{Im}(\omega_q)| < \kappa_1$). Interestingly, we find an oscillatory behavior $\Psi_q \sim e^{i\omega_q \log(-u)}$ for the outgoing flux observed at the future null infinity. However, if it decays rapidly (namely, $|\text{Im}(\omega_q)| > \kappa_1$), we obtain again the power-law behavior given by

$$\Psi_q(u) \sim (-u)^{\kappa_1}. \quad (4.17)$$

Then, no new feature appears for the time evolution of $\Psi(u)$, even if the quasi-normal mode is generated.

In summary, we have obtained various contributions to $\dot{a}_{\text{out}}(u)$ representing the outgoing flux observed at the retarded time u in terms of the decomposition of the Green's function as follows,

$$\dot{a}_{\text{out}} = \Psi_{F2} + \Phi + \Psi_{F1} + \Psi_+ + \sum_q \Psi_q, \quad (4.18)$$

where the unimportant contribution Ψ_- is neglected. According to the difference of the source region, they show different asymptotic behaviors in the limit $u \rightarrow 0$. The first two terms Ψ_{F2} and Φ due to outgoing waves originated on the past null cone $u' = u$ show the power-law behavior with the power index κ_2 , while the next two terms Ψ_{F1} and Ψ_+ with the source region near the past Cauchy horizon $v' = 0$ show the power-law behavior with the power index κ_1 . If slowly decaying quasi-normal modes are excited near the regular center, an oscillatory behavior with respect to the logarithmic time $\log|u|$ can appear in the final term $\sum_q \Psi_q$. The important point is whether or not these terms can induce a divergent energy flux in the limit $u \rightarrow 0$, at which the effect of formation of a naked singularity appears. In the next section we will define the relation of \dot{a}_{out} to the outgoing energy flux measured by distant observers and discuss the values of κ_2 , κ_1 and ω_q under specific self-similar models.

V. THE OUTGOING ENERGY FLUX

In the previous sections we have used the comoving null coordinates u and v for specifying the observation point. The metric component g_{uv} for the double null coordinates is written by

$$g_{uv} = \frac{t^2 e^{2\nu} (V^2 - 1)}{uv}. \quad (5.1)$$

The comoving coordinates become crucially different from the double null coordinates \bar{u} and \bar{v} used by a ‘‘static’’ observer present at a point sufficiently distant from the center, where we obtain $g_{\bar{u}\bar{v}} \simeq 1$. As was shown in [12], if the spacetime describing a self-similar collapse is smoothly matched to the Schwarzschild spacetime at the star's surface, the retarded (or advanced) time \bar{u} (or \bar{v}) becomes equal to the retarded (or advanced) Eddington-Finkelstein null coordinate near $\bar{u} = 0$ (or near $\bar{v} = 0$). Hence, in this section we evaluate the outgoing energy flux $F(\bar{u})$ per a unit time of \bar{u} , instead of u , which is important as a quantity measured by the static observer near the future null infinity. Near the future null infinity (namely, at $z \simeq z_2$), Eq. (5.1) leads to $g_{uv} \sim (|u|/v)^{\kappa_2 - 1}$, and we find the relation

$$|\bar{u}| \sim |u|^{\kappa_2}. \quad (5.2)$$

Hence the outgoing energy flux $F(\bar{u})$ is given by

$$F(\bar{u}) \propto \left(\frac{da_{\text{out}}}{d\bar{u}} \right)^2 \sim \left(\frac{u}{\bar{u}} \right)^2 \times \left(\frac{da_{\text{out}}}{du} \right)^2. \quad (5.3)$$

It is also remarkable that near the past null infinity corresponding to $z \simeq z_1$, we obtain $|\bar{v}| \sim |v|^{\kappa_1}$.

It is clear from Eq. (4.18) that the outgoing flux defined by da_{out}/du diverges in the limit $u \rightarrow 0$, because in general the parameters κ_1 and κ_2 become smaller than unity, as was mentioned in Eq. (4.6). For example, the first two terms

Ψ_{F_2} and Φ in Eq. (4.18) give the divergent term $|u|^{\kappa_2-1}$ to da_{out}/du , which will represent a result of prompt emission of outgoing waves (measured by the comoving time u) on the past null cone $u' = u$ in the range $v' > u$, where the coordinates u' and v' denote a source point for wave generation. However, the ratio u/\bar{u} of the two retarded times in Eq. (5.3) works as a red-shift factor in calculation of the energy flux defined by $F(\bar{u})$, and the Ψ_{F_2} and Φ contribution (denoted by $f_1(\bar{u})$) to $da_{\text{out}}/d\bar{u}$ remains finite even in the limit $\bar{u} \rightarrow 0$.

On the other hand the next two terms Ψ_{F_1} and Ψ_+ in Eq. (4.18) give the divergent term $|u|^{\kappa_1-1}$ to da_{out}/du . As was mentioned in the previous section, these terms will represent a result of the reflection of an ingoing flux propagating along the null line $v' = u \rightarrow 0$, where we obtain $|\bar{v}'| \sim |v'|^{\kappa_1}$ for the advanced time \bar{v}' of the static observer. Thus, the divergent term $|u|^{\kappa_1-1}$ may be interpreted as a blue-shift factor \bar{v}'/v' for ingoing waves propagating along the path $v' = u$ toward the center. Of course, the red-shift effect also becomes important when the reflected waves propagate to the future null infinity, and the Ψ_{F_1} and Ψ_+ contribution (denoted by f_2) to $da_{\text{out}}/d\bar{u}$ is given by

$$f_2(\bar{u}) \sim \frac{u}{\bar{u}} \times \frac{|u|^{\kappa_1}}{|u|} \sim |\bar{u}|^{\xi_0}, \quad \xi_0 = \frac{\kappa_1}{\kappa_2} - 1, \quad (5.4)$$

in the limit $\bar{u} \rightarrow 0$. If κ_2 is smaller than κ_1 , the contribution f_2 becomes zero rather than finite as $\bar{u} \rightarrow 0$, which contrasts with the limit of f_1 . This may mean that the red-shift of the reflected waves is more pronounced than that of the waves without passing through the center.

Let us denote wave frequencies for quasi-normal modes by $\omega_q = \omega_{Rq} + i\omega_{Iq}$ for real ω_{Rq} and ω_{Iq} . If $|\omega_{Iq}|$ is larger than κ_1 for all q , the Ψ_q contribution (denoted by f_{3q}) to $da_{\text{out}}/d\bar{u}$ shows the same power-law behavior as f_2 . We note that the amplification due to the blue-shift effect on the null line $v' = u$ can still work even for rapidly decaying quasi-normal modes. If $|\omega_{Iq}|$ becomes smaller than κ_1 for some q , the contribution f_{3q} in the limit $\bar{u} \rightarrow 0$ can be written by the oscillatory form

$$f_{3q}(\bar{u}) \sim |\bar{u}|^{\xi_q} \cos\left(\frac{\omega_{Rq}}{\kappa_2} \log |\bar{u}|\right), \quad \xi_q = \frac{|\omega_{Iq}|}{\kappa_2} - 1. \quad (5.5)$$

Owing to prompt generation of waves induced by slowly decaying quasi-normal modes in the range $u' < v' < u$, the blue-shift effect on the null line $v' = u$ becomes insignificant.

In conclusion, we find the asymptotic behavior (in the limit $\bar{u} \rightarrow 0$) of the outgoing energy flux $F(\bar{u})$ measured by static observers present near the future null infinity as follows,

$$F(\bar{u}) \propto \left(f_1(\bar{u}) + f_2(\bar{u}) + \sum_q f_{3q}(\bar{u}) \right)^2 \simeq \left\{ c_1 + c_2 |\bar{u}|^{\xi_0} + \sum_q c_3 |\bar{u}|^{\xi_q} \cos\left(\frac{\omega_{Rq}}{\kappa_2} \log |\bar{u}|\right) \right\}^2, \quad (5.6)$$

where c_1 , c_2 and c_3 are constants. The third term in Eq. (5.6) appears only if there exist quasi-normal modes satisfying the condition $|\omega_{Iq}| < \kappa_1$. By virtue of the red-shift effect no divergence of the energy flux $F(\bar{u})$ occurs even at the moment when the effect of naked singularity formation arrives at the future null infinity, unless κ_1 or $|\omega_{Iq}|$ becomes smaller than κ_2 . For the self-similar collapse such that κ_1 becomes smaller than $|\omega_{Iq}|$ and κ_2 , the power-law divergence

$$F(\bar{u}) \sim |\bar{u}|^{2\xi_0}, \quad (5.7)$$

will be observed as a dominant behavior with the power index limited to the range $-2 < 2\xi_0 < 0$. If slowly decaying quasi-normal modes are excited (namely, if $|\omega_{Iq}|$ is smaller than κ_1 and κ_2), the oscillatory divergence

$$F(\bar{u}) \sim |\bar{u}|^{2\xi_q} \cos^2\left(\frac{\omega_{Rq}}{\kappa_2} \log |\bar{u}|\right), \quad -2 < 2\xi_q < 0, \quad (5.8)$$

can become a more interesting precursor of naked singularity formation. Of course, the generation of a divergent energy flux means that the naked singularity formation is an unstable process against a backreaction of perturbations. Nevertheless the above-mentioned precursor phenomenon may significantly appear, before the backreaction effect becomes important. Even if $F(\bar{u})$ remains finite at $\bar{u} = 0$, the anomalous time evolution of $F(\bar{u})$ due to the damping term $|\bar{u}|^{\xi_0}$ or $|\bar{u}|^{\xi_q} \cos(\omega_{Rq} \log |\bar{u}|/\kappa_2)$ will appear in principle as an observable effect different from usual black hole formation.

Here we briefly comment on the outgoing energy flux in black hole formation in terms of Eq. (5.6). This corresponds to the case $V'(z_2) \rightarrow 0$ (namely, $z_m = z_2 = z_3$ in Fig. 1), for which the Cauchy horizon coincides with the event horizon. Then, the power indices ξ_0 and ξ_q become infinitely large, and the power law decay of the second and third terms in Eq. (5.6) will change to an exponential decay. The first term c_1 in Eq. (5.6) also vanishes in the limit

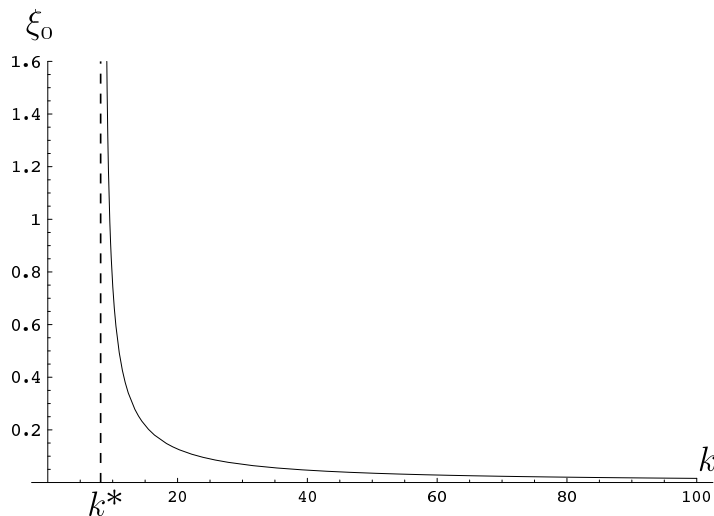


FIG. 4: Numerical evaluation of the power law index ξ_0 for dust collapse parameterized by k . The value of ξ_0 diverges at $k = k^*$, where the future Cauchy horizon coincides with the event horizon.

$V'(z_2) \rightarrow 0$, because the Jacobian $J(u, v')$ involved in the integrals (4.3) and (3.31) (giving Ψ_{F2} and Φ) is found to be proportional to the parameter $V'(z_2)$ at the leading order in the limit $u \rightarrow 0$, by considering the constant factor omitted in Eq. (4.4). The formula given by Eq. (5.6) can describe the infinite red-shift effect at the event horizon which makes the outgoing energy flux $F(\bar{u})$ completely vanish at $\bar{u} = 0$.

The key parameters for determining the asymptotic evolution of $F(\bar{u})$ are the ratios κ_1/κ_2 and $|\omega_{Iq}|/\kappa_2$. To discuss the values of the parameters, we must specify the self-similar model. If the collapsing matter is a perfect fluid, the self-similarity (2.2) is satisfied only for the equation of state $P = \alpha\rho$, and we find the inequality $\kappa_1 > \kappa_2$ for $0 \leq \alpha \leq 1$. The general proof of this inequality except the case $\alpha = 0$ is given in Appendix C. For the collapse of dust (namely, for $\alpha = 0$) we can obtain explicitly the metric (2.1) as follows,

$$\nu(z) = 0, \quad S(z) = \left\{ \frac{3}{2} \left(k - \frac{1}{z} \right) \right\}^{2/3}, \quad (5.9)$$

from which the function $V(z)$ is derived as

$$V(z) = ze^\lambda = \frac{1}{3} \left\{ \frac{9z}{4(kz - 1)} \right\}^{1/3} (3kz - 1), \quad (5.10)$$

where k is a positive constant. The global structure described in Fig. 2 (corresponding to the behavior of V shown in Fig. 1) is possible only in the range $k > k^* = (26 + 15\sqrt{3})/6 \simeq 8.7$, and from Fig. 4 it is easy to see that the power law index ξ_0 becomes always positive. Naked singularity formation due to self-similar collapse of a perfect fluid will not induce a divergent outgoing energy flux $F(\bar{u})$, unless there exist slowly decaying quasi-normal modes with $|\omega_{Iq}|/\kappa_2 < 1$. It will be interesting to check whether or not the inequality $\kappa_1 > \kappa_2$ holds for any other collapsing matter (for example, in the case of a scalar-field collapse).

To analyze the quasi-normal modes in general, it will be useful to rewrite the homogeneous equation for the outgoing mode $\psi_{\text{out}}(z, \omega)$ into an one-dimensional Schrödinger-type differential equation with a potential $U(z)$, which is given by the metric components ν , S and λ and decreases in proportion to $1 - V^2$ in the limit $z \rightarrow z_1$ (see Appendix B for the equation). The existence of the quasi-normal solution ψ_{out} satisfying the regularity at $z = 0$ is shown in Appendix D, by assuming some suitable form of U . We find the case such that the absolute value $|\omega_{Iq}|$ of the imaginary part of the complex frequency ω_q with nonzero ω_{Rq} can be smaller than κ_1 . However, it remains unclear whether or not such a case is possible for the metric satisfying the Einstein equations. This problem would be more extensively investigated in future works.

We have developed the Green's function technique to study time evolution of electromagnetic perturbations in the self-similar background, which will be applicable to any other test fields (for example, scalar and gravitational fields). We have also clarified that the various contributions to the Green's function (for example, high frequency part and quasi-normal modes) given by Eq. (4.18) are closely related to the difference of the source region where the corresponding perturbations are generated.

Our main result is the finding of the key parameters κ_1/κ_2 and $|\omega_{Iq}|/\kappa_2$ to determine the occurrence of divergent energy flux associated with naked singularity formation. The value of the complex quasi-normal frequency ω_q should depend not only on the background geometry but on the test field (and l parameterizing the field angular momentum). On the other hand, the values of κ_1 and κ_2 are purely geometrical quantities given by the derivative of the metric on the past and future Cauchy horizons, respectively. The blue-shift and red-shift effects defined by \bar{v}/v and u/\bar{u} for ingoing and outgoing waves propagating near the Cauchy horizons are parameterized by these geometrical quantities. The competition of such two effects in generation of outgoing energy flux would be an important feature of naked singularity.

It is interesting to compare our result with the result giving by Chandrasekhar and Hartle[22], who have considered time evolution of electromagnetic and gravitational perturbations inside the Reissner-Nordström black hole. The black hole contains a timelike singularity visible by a falling observer in the black hole. Estimating the energy flux received by an observer near the (future) Cauchy horizon for the timelike singularity, they have found that its amplitude has an exponential behavior with the rate $\kappa_- - \kappa_+$, where κ_+ and κ_- are the surface gravity factors evaluated on the event horizon and the Cauchy horizon, respectively (note that the event horizon corresponds to the past Cauchy horizon). Because the rate $\kappa_- - \kappa_+$ is always positive, the energy flux diverges when the observer arrives at the Cauchy horizon. The power index ξ_0 , which is written by the difference of the constant κ evaluated on the future and past Cauchy horizon by Eq. (2.11), resembles the rate, except that it is not always positive. This commonality would provide an important insight into an universal feature of perturbation response in various geometries with a naked singularity.

Further we would like to emphasize that the power index γ of the divergent energy flux $F \sim |\bar{u}|^\gamma$ with (or without) an oscillation (corresponding to $\gamma = 2\xi_q$ (or $\gamma = 2\xi_0$)) is allowed in the range $-2 < \gamma < 0$. This sharply contrasts with the semiclassical result giving the unique power index $\gamma = -2$ for the radiation of quantized test fields without depending on the parameters of the self-similar background[11, 12, 13, 14, 15, 16]. Such a difference of the power-law divergence may become an important clue for understanding profoundly quantum properties of perturbations around naked singularity.

APPENDIX A: APPLICATION TO MINKOWSKI BACKGROUND

Let us apply Eq. (3.18) to Minkowski background $\nu = \lambda = 0$ and $S = 1$ for checking the validity of the formulas given in Sec. III. Here we consider the dipole field with $l = 1$. Then, the homogeneous solutions for Eq. (3.4) are easily given by

$$g_{\text{out}}(z, \omega) = \omega - \frac{i}{z}, \quad g_{\text{in}}(z, \omega) = \omega + \frac{i}{z}. \quad (\text{A1})$$

Of course we obtain $b_1 = b_2 = 1$ for the coefficients in Eq. (3.11), and the Wronskian factor is given by

$$w(\omega) = 2i\omega(\omega + i)(\omega - i). \quad (\text{A2})$$

Then, from Eqs. (3.7), (3.19) and (3.20) we find

$$H(u, v|u', v') = \frac{2(uv + u'v') - (v' + u')(v + u)}{(v - u)(v' - u')(v' + u')}, \quad (\text{A3})$$

for $u < v'$, and $H(u, v|u', v') = 0$ for $v' < u$. To calculate explicitly Eq. (3.18), we assume the shell-like current distribution $j_1(t, z) = j_0\delta(r - r_0)$ for a constant j_0 . Then, we find $a(r) = -4\pi j_0 r_0^2/3r$ for $r > r_0$, and $a(r) = -4\pi j_0 r^2/3r_0$ for $r < r_0$. This corresponds to the vector potential for a static dipole magnetic field.

APPENDIX B: ANALYSIS OF HOMOGENEOUS SOLUTIONS

Here we analyze the homogeneous solutions $\psi(z, \omega)$ for Eq. (3.4), by rewriting it into the one-dimensional Schrödinger-type differential equation

$$\frac{d^2\tilde{\psi}}{dx^2} + (\omega^2 - U(x))\tilde{\psi} = 0, \quad (\text{B1})$$

where the new variable x and the “potential” U are given by

$$x = \frac{1}{2}(h_{\text{out}}(z) - h_{\text{in}}(z)), \quad (\text{B2})$$

and

$$U(x) = \frac{l(l+1)e^{2\nu}(1-V^2)}{S^2z^2}. \quad (\text{B3})$$

Note that $U > 0$ in the region I shown in Fig. 2. The function $\tilde{\psi}$ is defined by

$$\tilde{\psi}(x, \omega) \equiv \psi(z, \omega)e^{-i\omega(h_{\text{out}}(z)+h_{\text{in}}(z))/2}. \quad (\text{B4})$$

To obtain the homogeneous solutions giving ψ_0 and ψ_{out} , we must consider the behavior at the points $z = 0$ and $z = z_1$ corresponding to $x = 0$ and $x = \infty$, respectively. The local flatness at the regular center and the suitable gauge choice allow us, without loss of generality, to assume that $\nu \simeq 0$ and $e^\lambda \simeq mS \simeq C_\lambda(-z)^{m-1}$ near $z = 0^1$, where C_λ and m are positive constants. Then, we find the approximate form

$$U(x) \simeq \frac{l(l+1)}{x^2}, \quad (\text{B5})$$

near $x = 0$. On the other hand it is easy to see that

$$U(x) \simeq U_\infty e^{-2\kappa_1 x}, \quad (\text{B6})$$

in the limit $x \rightarrow \infty$, where U_∞ is a positive constant. It is remarkable that we have $U = l(l+1)/\sinh^2 x$ and $z = -\tanh x$ for the Minkowski metric.

Denoting the solutions for Eq. (B1) by $\tilde{\psi}_{\text{out}}$ and $\tilde{\psi}_{\text{in}}$ corresponding to ψ_{out} and ψ_{in} , respectively, we obtain

$$\tilde{\psi}_{\text{out}}(x, \omega) = g_{\text{out}}(z, \omega)e^{i\omega x}, \quad \tilde{\psi}_{\text{in}}(x, \omega) = g_{\text{in}}(z, \omega)e^{-i\omega x}. \quad (\text{B7})$$

The approximate forms of these functions for large x are given by

$$g_{\text{out}}(x, \omega) \simeq g_{\text{out}}^\infty(\omega) \left\{ 1 + \frac{U_\infty}{4\kappa_1(\kappa_1 - i\omega)} e^{-2\kappa_1 x} \right\}, \quad (\text{B8})$$

and

$$g_{\text{in}}(x, \omega) \simeq g_{\text{in}}^\infty(\omega) \left\{ 1 + \frac{U_\infty}{4\kappa_1(\kappa_1 + i\omega)} e^{-2\kappa_1 x} \right\}, \quad (\text{B9})$$

for some functions g_{out}^∞ and g_{in}^∞ dependent on ω . To keep these functions well-defined even at $\omega = \pm\kappa_1 i$, the functions g_{out}^∞ and g_{in}^∞ are required to contain the factor $\kappa_1 - i\omega$ and $\kappa_1 + i\omega$, respectively. Then, we obtain $w(\omega) = 2i\omega g_{\text{out}}^\infty g_{\text{in}}^\infty = 0$ at $\omega = \pm\kappa_1 i$, for which it is easy to see that the two modes $\tilde{\psi}_{\text{out}}$ and $\tilde{\psi}_{\text{in}}$ become linearly dependent at the leading order in the limit $x \rightarrow \infty$.

Next, using Eq. (B1), we prove that the imaginary part of the frequencies ω_q of quasi-normal modes denoted by $\tilde{\psi}_q(x)$ should be negative. We require the boundary conditions for the quasi-normal modes such that $\tilde{\psi}_q \sim x^{l+1}$ near $x = 0$, and $\tilde{\psi}_q \sim e^{i\omega_q x}$ in the limit $x \rightarrow \infty$. Then, integrating Eq. (B1) multiplied by the complex conjugate $\tilde{\psi}_q^*$ in the range $0 \leq x \leq x_0$, where x_0 is a positive constant satisfying $\tilde{\psi}_q(x_0, \omega_q) \neq 0$, for sufficiently large x_0 we obtain

$$X\omega_q^2 + i\omega_q Y - Z = 0, \quad (\text{B10})$$

where the coefficients given by

$$X = \int_0^{x_0} |\tilde{\psi}_q|^2 dx, \quad Y = |\tilde{\psi}_q(x_0)|^2, \quad Z = \int_0^{x_0} \left(\left| \frac{d\tilde{\psi}_q}{dx} \right|^2 + U |\tilde{\psi}_q|^2 \right) dx, \quad (\text{B11})$$

are positive definite. It is easy to see that $\text{Im}(\omega_q) = -Y/2X < 0$ for $4XZ > Y^2$, and $\text{Im}(\omega_q) = -(Y \pm \sqrt{Y^2 - 4XZ})/2X < 0$ for $4XZ < Y^2$.

¹ Then, via the coordinate transformation $\hat{r} = r^{1+m}$, we can find that near $z = 0$,

$$ds^2 \simeq -dt^2 + \left\{ \frac{C_\lambda(-t)^{1-m}}{m} \right\}^2 (d\hat{r}^2 + \hat{r}^2 d\Omega^2).$$

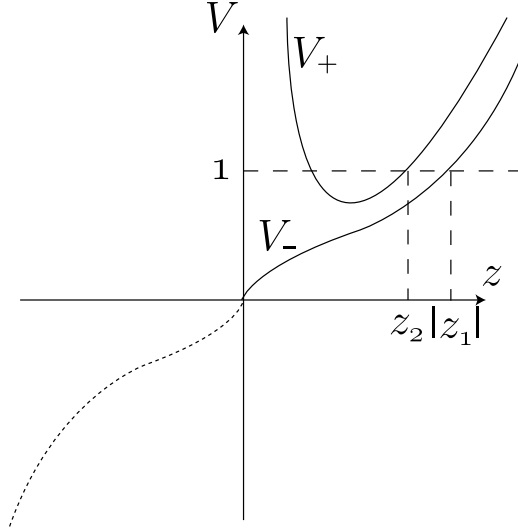


FIG. 5: Schematic description (solid lines) of the functions $V_+(z)$ and $V_-(z)$. The dotted line denotes the function $V(z)$ for $z < 0$. The line $V = V_-(z)$ is the point symmetric line to the dotted line with respect to the origin.

APPENDIX C: PERFECT FLUID COLLAPSE WITH PRESSURE

In this appendix, we prove that the value of κ_2 is always smaller than that of κ_1 in the spacetime describing the collapse of a perfect fluid with the equation of state $P = \alpha\rho$ for $0 < \alpha \leq 1$. For convenience, we express the function $V(z)$ for $z > 0$ and the point symmetric function to the function $V(z)$ for $z < 0$ concerning the origin $(z, V) = (0, 0)$ by the notation $V_+(z)$ and $V_-(z)$, respectively (see Fig. 5). As stated in [20], the function $V_-(z)$ is also given by the metric satisfying the Einstein equations. In addition, we define $\dot{\equiv} zd/dz$ only in this appendix. Hence, what we show is that the value of $\dot{V}_+(z_2)$ is always smaller than that of $\dot{V}_-(|z_1|)$.

Now we start the proof with a similar notation used by Carr and Coley in [20]. They introduced the functions $A(z)$ and $B(z)$ defined by $(4\pi\rho r^2)^{-\alpha/(1+\alpha)} = A_0 e^{A(z)}$ and $S(z) = B_0 e^{B(z)}$ for positive constants A_0 and B_0 . From the Einstein equations, the functions $\nu(z)$ and $\lambda(z)$ can be expressed in terms of the functions $A(z)$ and $B(z)$. Hence, the function $V(z)$ for $z > 0$ can be expressed as

$$V(z) = V_0 B_0^{-2} z^{(1-\alpha)/(1+\alpha)} e^{-2B+A(1-\alpha)/\alpha}, \quad (\text{C1})$$

for a positive constant V_0 (see Eq. (2.19) of [20]). In addition, we use one of the Einstein equations

$$V^2 \left(\dot{B} - \frac{\dot{A}}{2\alpha} \right) = -\frac{\dot{A}}{2} + \left(\frac{\alpha}{1+\alpha} \right) \left\{ e^{-4B+A(1-\alpha)/\alpha} - 1 \right\}, \quad (\text{C2})$$

which is shown in Eq. (4.23) of [20]. When $V = 1$, Eqs. (C1) and (C2) give

$$\dot{V} = 1 - \frac{2\alpha}{1+\alpha} e^{-4B+A(1-\alpha)/\alpha}. \quad (\text{C3})$$

This means that the values of $\dot{V}_-(z)$ and $\dot{V}_+(z)$ at $z = |z_1|$ and $z = z_2$, respectively, become

$$\dot{V}_-(|z_1|) = 1 - \frac{2\alpha}{V_0(1+\alpha)} |z_1|^{-(1-\alpha)/(1+\alpha)} S^{-2}(z_1), \quad (\text{C4})$$

and

$$\dot{V}_+(z_2) = 1 - \frac{2\alpha}{V_0(1+\alpha)} z_2^{-(1-\alpha)/(1+\alpha)} S^{-2}(z_2). \quad (\text{C5})$$

As stated in [20], the solution describes the monotonical collapse. This means that the value of $S(z_1)$ is larger than that of $S(z_2)$. Hence, when $\alpha = 1$, we find the inequality $\dot{V}_+(z_2) < \dot{V}_-(|z_1|)$ from Eqs. (C4) and (C5). On the other

hand, for $0 < \alpha < 1$, Eqs. (C4) and (C5) indicate that if the value $|z_1|$ is larger than the value z_2 , the value of $\dot{V}_+(z_2)$ is always smaller than that of $\dot{V}_-(|z_1|)$. The condition $|z_1| > z_2$ is satisfied if the inequality $V_+(z) > V_-(z)$ holds for the whole region $z \geq |z_1|$, as depicted in Fig. 5. Therefore, the remaining problem is to show the inequality $V_+(z) > V_-(z)$ in the whole region $z \geq |z_1|$ for $0 < \alpha < 1$.

We firstly show that $V_+(z) > V_-(z)$ holds at the sufficiently large z . By requiring the left hand side of Eq. (C2) to be finite as $V \rightarrow \infty$, we find that at the sufficiently large z , Eq. (C2) becomes

$$\dot{B} = \frac{\dot{A}}{2\alpha}, \quad (\text{C6})$$

which is also shown in Eq. (4.25) of [20]. From this equation and Eq. (C1), we can obtain

$$\frac{\dot{V}}{V} = \frac{1-\alpha}{1+\alpha} - 2\alpha\dot{B}. \quad (\text{C7})$$

Hence, we find

$$\frac{V'_-}{V_-} - \frac{V'_+}{V_+} = -2\alpha(B'_- - B'_+), \quad (\text{C8})$$

where the functions $B_-(z)$ and $B_+(z)$ denote the values of $B(z)$ along the lines of $V(z) = V_-(z)$ and $V(z) = V_+(z)$, respectively. The monotonical collapse also means that $B'_- < 0$ and $B'_+ > 0$. In addition, the equality $V_+(z) = V_-(z)$ holds in the limit $z \rightarrow \infty$. These facts means that the inequality $V'_-(z) > V'_+(z)$ holds. Hence, the inequality $V_+(z) > V_-(z)$ holds at the sufficiently large z .

Next, we show that the lines $V = V_+(z)$ and $V = V_-(z)$ do not cross each other in the region $z > |z_1|$ to complete the proof. We eliminate the functions $A(z)$ and $\dot{A}(z)$ from Eq. (C2), using the function $V(z)$ and $\dot{V}(z)$, and obtain

$$\frac{\alpha}{1-\alpha}(1-V^2)\dot{B} = \frac{\alpha}{1+\alpha}\left(V_0^{-1}B_0^2z^{(\alpha-1)/(\alpha+1)}Ve^{-2B} - 1\right) - \frac{1}{2}(\alpha - V^2)\left(\frac{\dot{V}/V}{1-\alpha} - \frac{1}{1+\alpha}\right). \quad (\text{C9})$$

We consider the difference between Eq. (C9) expressed in terms of $V_-(z)$ and $B_-(z)$ and Eq. (C9) expressed in terms of $V_+(z)$ and $B_+(z)$. Then, for the region $V_+ \geq 1$ and $V_- \geq 1$, we can find the inequality

$$\begin{aligned} & \left(V_- - \frac{\alpha}{V_-}\right)\dot{V}_- - \left(V_+ - \frac{\alpha}{V_+}\right)\dot{V}_+ \\ & > \frac{1-\alpha}{1+\alpha}\left\{V_-^2 - V_+^2 + 2\alpha V_0^{-1}B_0^2z^{(\alpha-1)/(\alpha+1)}(V_+e^{-2B_+} - V_-e^{-2B_-})\right\}, \end{aligned} \quad (\text{C10})$$

because of the conditions $\dot{B}_- < 0$ and $\dot{B}_+ > 0$. Now we assume that the lines $V = V_+(z)$ and $V = V_-(z)$ cross each other (i.e., $V_+(z) = V_-(z) = V_c \geq 1$) at some points z . At this point, the inequality (C10) becomes

$$\left(V_c - \frac{\alpha}{V_c}\right)(\dot{V}_- - \dot{V}_+) > \frac{2V_0^{-1}B_0^2V_c\alpha(1-\alpha)}{1+\alpha}z^{(\alpha-1)/(\alpha+1)}(e^{-2B_+} - e^{-2B_-}). \quad (\text{C11})$$

Because of the monotonical collapse condition $B_-(z) > B_+(z)$, we obtain the inequality $\dot{V}_-(z) > \dot{V}_+(z)$. However, since the inequality $V_+(z) > V_-(z)$ holds at the sufficiently large z , the derivatives should satisfy $\dot{V}_+(z) \geq \dot{V}_-(z)$ at the point where $V_+(z) = V_-(z)$. This is a contradiction, which is solved by denying the existence of the point where $V_+(z) = V_-(z)$. Hence, the inequality $V_+(z) > V_-(z)$ holds in the whole region $V_-(z) \geq 1$. This conclusion ends the proof that the inequality $\dot{V}_+(z_2) < \dot{V}_-(|z_1|)$ always holds for $0 < \alpha \leq 1$.

APPENDIX D: APPROXIMATE EVALUATION OF FREQUENCIES OF QUASI-NORMAL MODES

The oscillatory behavior shown by Eq. (5.5) can appear if there exist quasi-normal modes with the frequencies ω_q satisfying the conditions $\text{Re}(\omega_q) \neq 0$ and $|\text{Im}(\omega_q)| < \kappa_1$, though it depends on the value of κ_2 whether or not the divergence of the energy flux occurs. In general it will be a difficult task to find quasi-normal modes as homogeneous solutions for Eq. (3.4) constructed by self-similar metrics satisfying the Einstein equations. Even the existence of such modes will be unclear. Hence, in this appendix we consider a simple form of the potential $U(x)$ defined by Eq. (B3).

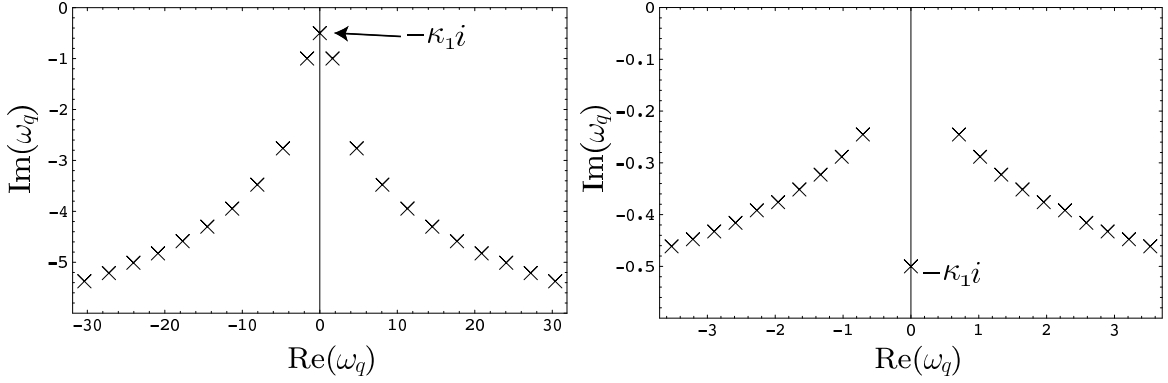


FIG. 6: The complex frequencies ω_q of quasi-normal modes for the potential $U(x)$ given by Eq. (D1). The left and right panels correspond to the cases $x_c = 1$ and $x_c = 10$, respectively, while the other parameters are fixed to be $l = 1$, $U_\infty = 8$ and $\kappa_1 = 0.5$.

Our purpose is to illustrate that only a slight modification of U from the potential given by the Minkowski metric is sufficient for obtaining quasi-normal modes.

Taking account of the asymptotic behaviors given by Eqs. (B5) and (B6), we can give a plausible approximation of U by

$$U(x) = \begin{cases} \frac{l(l+1)}{x^2} & \text{for } x \leq x_c, \\ \frac{\zeta + (U_\infty - \zeta)(1 - e^{-2\kappa_1 x})}{4 \sinh^2(\kappa_1 x)} & \text{for } x \geq x_c, \end{cases} \quad (\text{D1})$$

where ζ and x_c are constants. Because the potential should be continuous at $x = x_c$, the parameter ζ is given by

$$\zeta = e^{2\kappa_1 x_c} \left\{ \frac{4l(l+1) \sinh^2(\kappa_1 x_c)}{x_c^2} - U_\infty (1 - e^{-2\kappa_1 x_c}) \right\}. \quad (\text{D2})$$

Therefore the potential U given by Eq. (D1) is parameterized by l , x_c , U_∞ and κ_1 .

From the regularity of quasi-normal modes denoted by $\tilde{\psi}_q$ at $x = 0$, we obtain for $x \leq x_c$

$$\tilde{\psi}_q(x) = \sqrt{x} J_{l+(1/2)}(\omega_q x), \quad (\text{D3})$$

where $J_{l+(1/2)}$ denotes the Bessel function. On the other hand, from the asymptotic behavior $\tilde{\psi}_q \sim e^{i\omega_q x}$, we obtain for $x \geq x_c$

$$\tilde{\psi}_q(x) = g_{\text{out}}^\infty(\omega_q) (1 - e^{-2\kappa_1 x})^\mu F\left(\beta_1, \beta_2, 1 - \frac{i\omega}{\kappa_1}; e^{-2\kappa_1 x}\right) e^{i\omega_q x}, \quad (\text{D4})$$

where $\mu = \{1 + \sqrt{1 + (\zeta/\kappa_1)}\}/2$, and F is the hypergeometric function with β_1 and β_2 given by

$$\beta_1 \beta_2 = \frac{U_\infty}{4\kappa_1^2} - \mu \left(\frac{i\omega}{\kappa_1 - 1} \right), \quad (\text{D5})$$

and

$$\beta_1 + \beta_2 = 2\mu - \frac{i\omega}{\kappa_1}. \quad (\text{D6})$$

By requiring that the functions given by Eqs. (D3) and (D4) are smoothly matched at $x = x_c$, we can find the frequencies ω_q . The numerical results are illustrated in Fig. 6. We can confirm that there are a number of quasi-normal modes with $\text{Re}(\omega_q) \neq 0$. Further the dependence of the minimum value (denoted by $|\text{Im}(\omega_0)|$) of $|\text{Im}(\omega_q)|$ on the parameters can be summarized as follows. (1) The value of $|\text{Im}(\omega_0)|$ decreases as x_c increases, and it becomes equal to κ_1 for a certain value of x_c in the range $1 \leq x_c \leq 10$ for the parameter values used in Fig. 6. (2) Even for

$x_c = 1$ it can become smaller than κ_1 as the ratio U_∞/κ_1 increases. For example, we obtain $|\text{Im}(\omega_0)| \simeq 0.183$ for $U_\infty = 40$, $\kappa_1 = 0.5$ and $x_c = l = 1$. We can claim that the conditions $\text{Re}(\omega_q) \neq 0$ and $|\text{Im}(\omega_q)| < \kappa_1$ are satisfied in a wide range of the parameter values.

-
- [1] R. Penrose, Riv. Nuovo Cimento **1**, 252 (1969).
 - [2] T. Harada, Pramana **53**, 1 (1999), gr-qc/0407109.
 - [3] T. Harada, H. Iguchi, and K. Nakao, Prog. Theor. Phys. **107**, 449 (2002), gr-qc/0204008.
 - [4] T. P. Singh and P. S. Joshi, Class. Quantum Grav. **13**, 559 (1996).
 - [5] S. Jhingan, P. S. Joshi, and T. P. Singh, Class. Quantum Grav. **13**, 3057 (1996), gr-qc/9604046.
 - [6] A. Ori and T. Piran, Phys. Rev. D **42**, 1068 (1990).
 - [7] T. Foglizzo and R. N. Henriksen, Phys. Rev. D **48**, 4645 (1993).
 - [8] B. J. Carr and C. Gundlach, Phys. Rev. D **67**, 024035 (2003), gr-qc/0209092.
 - [9] B. J. Carr, A. A. Coley, M. Goliath, U. S. Nilsson, and C. Uggla, Class. Quant. Grav. **18**, 303 (2001), gr-qc/9902070.
 - [10] T. Harada and H. Maeda, Phys. Rev. D **63**, 084022 (2001), gr-qc/0101064.
 - [11] W. A. Hiscock, L. G. Williams, and D. M. Eardley, Phys. Rev. D **26**, 751 (1982).
 - [12] S. Barve, T. P. Singh, C. Vaz, and L. Witten, Nucl. Phys. **B532**, 361 (1998), gr-qc/9802035.
 - [13] S. Barve, T. P. Singh, C. Vaz, and L. Witten, Phys. Rev. D **58**, 104018 (1998), gr-qc/9805095.
 - [14] C. Vaz and L. Witten, Phys. Lett. B **442**, 90 (1998), gr-qc/9804001.
 - [15] T. P. Singh and C. Vaz, Phys. Lett. B **481**, 74 (2000), gr-qc/0002018.
 - [16] U. Miyamoto and T. Harada, Phys. Rev. D **69**, 104005 (2004), gr-qc/0312080.
 - [17] B. C. Nolan and T. J. Waters, Phys. Rev. D **66**, 104012 (2002), gr-qc/0210035.
 - [18] C. T. Cunningham, R. H. Price, and V. Moncrief, Astrophys. J. **224**, 643 (1978).
 - [19] B. J. Carr and A. A. Coley, Class. Quant. Grav. **16**, R31 (1999), gr-qc/9806048.
 - [20] B. J. Carr and A. A. Coley, Phys. Rev. D **62**, 044023 (2000), gr-qc/9901050.
 - [21] B. J. Carr, Phys. Rev. D **62**, 044022 (2000), gr-qc/0003007.
 - [22] S. Chandrasekhar and J. B. Hartle, Proc. R. Soc. London **A384**, 301 (1982).